ISSN 0036-0236, Russian Journal of Inorganic Chemistry, 2009, Vol. 54, No. 11, pp. 1779–1788. © Pleiades Publishing, Inc., 2009.
Original Russian Text © T.A. Rodina, A.V. Ivanov, V.A. Konfederatov, V.I. Mitrofanova, A.V. Gerasimenko, O.N. Antzutkin, 2009, published in Zhurnal Neorganicheskoi Khimii, 2009, Vol. 54, No. 11, pp. 1858–1867.

Synthesis, Structure, and ^{13}C and ^{31}P CP/MAS NMR of Crystalline Modifications of the Polynuclear Thallium(I) *O,O'*-Dicyclohexyl Phosphorodithioate Complex $[Tl\{S_2P(O\text{-}cyclo\text{-}C_6H_{11})_2\}]_n$

T. A. Rodina[a], A. V. Ivanov[b], V. A. Konfederatov[b], V. I. Mitrofanova[a], A. V. Gerasimenko[c], and O. N. Antzutkin[d]

[a] *Amur State University, Ignat'evskoe sh. 21, Blagoveshchensk, 675027 Russia*
[b] *Institute of Geology and Nature Management, Far East Division, Russian Academy of Sciences, Relochnyi per. 1, Blagoveshchensk, 675000 Russia*
[c] *Institute of Chemistry, Far East Division, Russian Academy of Sciences, pr. Stoletiya Vladivostoka 159, Vladivostok, 690022 Russia*
[d] *Luleå University of Technology, S-971 87 Luleå, Sweden; University of Wazwick, CV47AL, Coventry, UK*
E-mail: alexander.v.ivanov@chemist.com

Received May 20, 2008

Abstract—Two crystalline modifications (**Ia** and **Ib**) of the polynuclear thallium (I) *O,O'*-dicyclohexyl phosphorodithioate complex $[Tl\{S_2P(O\text{-}cyclo\text{-}C_6H_{11})_2\}]_n$ have been synthesized and characterized by CP/MAS NMR (^{13}C, ^{31}P). From full ^{31}P CP/MAS NMR spectra, the χ^2 plots were constructed to calculate the ^{31}P chemical shift anisotropy $^{31}P - \delta_{aniso} = (\delta_{zz} - \delta_{iso})$ and asymmetry parameters $\eta = (\delta_{yy} - \delta_{xx})/(\delta_{zz} - \delta_{iso})$. The data obtained for the *O,O'*-dicyclohexyl phosphorodithioate (Dtph) groups (in both modifications) are evidence that the ^{31}P chemical shift tensors are intermediate between rhombic and axially symmetric. However, whereas the rhombic component dominates for **Ia**, the tensor for **Ib** is close to axially symmetric (for $\delta_{zz} < \delta_{yy} \approx \delta_{xx}$). The same pattern of the MAS spectra corresponding to negative δ_{aniso} ($\delta_{zz} < \delta_{yy} < \delta_{xx}$) points to a bridging or terminal/bridging coordination mode of the Dtph groups. X-ray crystallography shows that complex **Ib** has a polynuclear structure (of the chain polymer type). The chains are composed of alternating structurally nonequivalent noncentrosymmetric binuclear molecules $[Tl_2\{S_2P(O\text{-}cyclo\text{-}C_6H_{11})_2\}_2]$. All Dtph ligands have the terminal/μ_3-bridging coordination mode.

DOI: 10.1134/S0036023609110138

In complexes with dithio derivatives, thallium(I) has high coordination numbers: CN = 5 [1–4], 6 [1, 4–7], and even 7 [8, 9]. Therefore, one ligand cannot coordinatively saturate the central atom and, in the compounds under consideration, this conflict is resolved by the formation of polynuclear structures (chain polymers of different types of structural organization). The basic structural units in *N,N*-dialkyldithiocarbamate complexes are binuclear molecules $[Tl_2(S_2CNR_2)_2]$, which are combined in chains, and the latter form layers. In this context, of interest are thallium(I) complexes with another group of S,S'-bidentate dithio derivatives, namely, with *O,O'*-dialkyl phosphorodithioate ions.

This work deals with the synthesis and comparative study of two crystalline modifications of the polynuclear thallium(I) *O,O'*-dicyclohexyl phosphorodithioate complex $[Tl\{S_2P(O\text{-}cyclo\text{-}C_6H_{11})_2\}]_n$ (**Ia**, **Ib**) by CP/MAS NMR (^{13}C, ^{31}P). The polynuclear structure of **Ib** (of the chain polymer type), which contains terminal/μ_3-bridging Dtph groups, was determined by X-ray crystallography.

EXPERIMENTAL

Synthesis of thallium(I) *O,O'*-dicyclohexyl phosphorodithioate $[Tl\{S_2P(O\text{-}cyclo\text{-}C_6H_{11})_2\}]_n$ (**Ia**): to a solution containing 0.40 g (0.0015 mol) of $TlNO_3$ (Merck) in 25 mL of water and acidified with two drops of nitric acid, a solution of 0.53 g (0.0016 mol) of $K\{S_2P(O\text{-}cyclo\text{-}C_6H_{11})_2\}$ in 25 mL of water was added under vigorous stirring. A bulky white precipitate was filtered off, washed with a small amount of water, and dried in air. The yield was 89%. Needle-shaped crystals of *catena*-poly[(μ_3-(*O,O'*-di-*cyclo*-hexylphosphorodithioato-*S,S,S,S'*)thallium(I)] $[Tl_2\{S_2P(O\text{-}cyclo\text{-}C_6H_{11})_2\}_2]_n$ (**Ib**) were obtained by recrystallization of **Ia** from acetone. According to elemental analysis data[1]:

---

[1] Elemental analysis was carried out by HR-ICP-MS (high-resolution inductively coupled plasma mass spectrometry) in the medium resolution range, $\Delta m/m \approx 4500$ (Finnigan MAT, Bremen, Germany).

For $TlS_2PO_2C_{12}H_{22}$ (FW = 497.76) anal. calcd. (%): S, 12.88; P, 6.22.

Found (%): S, 12.98; P, 6.25.

Compounds **Ia** and **Ib** and the initial potassium dicyclohexyl phosphorodithioate were characterized by ^{13}C CP/MAS NMR:

$[Tl\{S_2P(O\text{-}cyclo\text{-}C_6H_{11})_2\}]_n$ (**Ia**) (ppm): (1 : 2 : 2 : 1) 80.3, 72.9 (1 : 1, –OCH=); 35.2, 33.7, 31.5 (*o*-CH_2–); 26.6, 25.9 (*m*-CH_2–); 22.1 (*p*-CH_2–).

$[Tl_2\{S_2P(O\text{-}cyclo\text{-}C_6H_{11})_2\}_2]_n$ (**Ib**) (ppm): (1 : 2 : 3) 77.0, 76.5 (1 : 1, –OCH=); 36.4 (*o*-CH_2–); 26.6 (*m*-CH_2–); 27.6 (*p*-CH_2–).

$K\{S_2P(O\text{-}cyclo\text{-}C_6H_{11})_2\}$ (ppm): (1 : 2 : 3) 79.9, 78.8, 78.1, 77.1 (1 : 1 : 1 : 1, –OCH=); 35.7, 35.2, 34.7, 33.9 (*o*-CH_2–), 26.2 (*m*-, *p*-CH_2–).

CP/MAS NMR spectra (^{13}C, ^{31}P) were recorded on a Varian/Chemagnetics InfinityPlus CMX-360 spectrometer operating at 90.52 and 145.73 MHz, respectively (B_0 = 8.46 T, superconducting magnet, Fourier transform). Proton cross polarization was used for recording the spectra. To suppress ^{13}C–^{1}H and ^{31}P–^{1}H dipole–dipole interactions, CW decoupling at the proton resonance frequency was used [10]. Samples of the complexes (~350 mg) were placed in a zirconia rotor 7.5 mm in diameter. The ^{13}C/^{31}P NMR spectra were measured under magic angle spinning conditions at spinning frequencies of 2350–3150/2300–4500(1) Hz; the number of scans was 2900–7900/128–1400; the proton $\pi/2$ pulse width was 4.5/5.5–7.0 μs; the ^{1}H–^{13}C/^{1}H–^{31}P mixing time was 2.0/2.0–3.0 ms; the repetition time was 3.5/2.0–3.0 s. The isotropic ^{13}C NMR chemical shifts were measured in ppm from one of the components of the spectrum of crystalline adamantane as an external reference [11] (δ = 38.48 ppm from tetramethylsilane [12]); the ^{31}P NMR chemical shifts were referenced to aqueous 85% H_3PO_4 [13]. The homogeneity of the magnetic field was monitored by measuring the width of the reference signal of crystalline adamantane, which was 2.6 Hz. The isotropic chemical shifts were corrected for the magnetic field drift in the course of experiments, which constituted 0.051/0.11 Hz/h on the frequency scale for ^{13}C/^{31}P nuclei. To refine the chemical shifts and integrated intensity ratios for overlapping signals in ^{13}C NMR spectra, spectra were simulated piecewise taking into account the line position and width, as well as the Lorentzian and Gaussian contributions to the line shape. The ^{31}P chemical shift anisotropy ($\delta_{aniso} = \delta_{zz} - \delta_{iso}$) and the asymmetry parameter ($\{\eta = (\delta_{yy} - \delta_{xx})/(\delta_{zz} - \delta_{iso})\}$) were calculated using χ^2 plots [14], which were constructed based on the quantification of the spinning sideband integrated intensity ratios [15, 16] in the full ^{31}P CP/MAS NMR spectra recorded at two spinning frequencies. Calculations were performed with the Mathematica program [17].

The X-ray diffraction experiment was carried out at room temperature on a Bruker SMART 1000 CCD diffractometer (MoK_α radiation, graphite monochromator). Experimental intensity data were collected by a routine procedure in a hemisphere; the crystal–detector distance was 45 mm. Intensity data were corrected for absorption based on the indices of the single crystal facets. The structure was solved by direct methods and refined by least-squares calculation in the anisotropic approximation for non-hydrogen atoms. Hydrogen atoms were introduced in the geometrically calculated positions and refined as riding of their bonded carbon atoms.

Data collection and editing, as well as the refinement of unit cell parameters, were performed with the SMART and SAINT Plus program packages [18]. All calculations concerning structure solution and refinement were performed with the SHELXTL/PC program package [19]. Selected crystallographic data and refinement results for **Ib** are summarized in Table 1; atomic coordinates are presented in Table 2; and bond lengths and angles are listed in Table 3.

RESULTS AND DISCUSSION

The CP/MAS ^{13}C NMR spectra of thallium(I) dicyclohexyl phosphorodithioate samples—precipitated from an aqueous phase (**Ia**) and obtained by crystallization from acetone (**Ib**)—show resonance signals due to the Dtph ligands: the signals caused by the less shielded carbon nuclei in the –OCH= groups and more shielded carbon nuclei in the *o*-CH_2–, *m*-CH_2–, and *p*-CH_2– groups (Fig. 1). However, comparative analysis of these spectra in the region of each of the above groups demonstrates spectral difference between the samples of **Ia** and **Ib**.

In the center of gravity of the ^{31}P CP/MAS NMR spectrum of **Ia** (Fig. 2, a and a'), there is one signal (centerband) with the isotropic chemical shift (Table 4). The recrystallization of the complex from acetone leads to a new ^{31}P CP/MAS NMR spectrum (Fig. 2, b and b′). Despite a considerable similarity of these spectra (Fig. 2, a and a' and Fig. 2, b and b′), the isotropic chemical shift of the phosphorus sites of crystalline form **Ib** is noticeably higher than that for **Ia** (Table 4) while its width is almost twice as large as that of the latter. Thus, thallium(I) dicyclohexyl phosphorodithioate is able to exist in two modifications. Comparison of the ^{31}P isotropic chemical shifts for **Ia**, **Ib**, and initial potassium dicyclohexyl phosphorodithioate [20] allows us to state that covalent bonding of the Dtph groups is accompanied by a decrease in $\delta(^{31}P)$ and, hence, by an increase in the degree of electron shielding of ^{31}P nuclei. (The latter is consistent with our findings on dialkyl phosphorodithioate complex of some metals, such as nickel(II) [21], zinc(II) [22], cadmium(II) [23, 24], lead(II) [25, 26], silver(I) [27], and antimony(V) [28].) The lower ^{31}P isotropic chemical shift for **Ia** ($\delta = 93.5$ ppm) as compared to that for **Ib** ($\delta = 96.7$ ppm) is evidence of the stronger bonding of the Dtph groups in **Ia**.

As a rule, crystallization of complexes from organic solvents leads to a noticeable narrowing of ^{31}P NMR signals of phosphorodithioate complexes. The opposite situation occurs in our case: the ^{31}P NMR signal of **Ib** (lw = 219 Hz) is considerably broader than the signal of **Ia** (lw = 131 Hz) (lw is the line width). The latter can be evidence that **Ib** contains several nonequivalent Dtph groups with the same structural function.

For compounds **Ia** and **Ib**, the patterns of the full ^{31}P CP/MAS NMR spectra correspond to ^{31}P chemical shift tensors of the Dtph groups intermediate between rhombic and axially symmetric. However, whereas the rhombic component dominates for **Ia**, the tensor for **Ib** is close to axially symmetric (for $\delta_{zz} < \delta_{yy} \approx \delta_{xx}$). The same pattern of the MAS spectra corresponding to negative δ_{aniso} ($\delta_{zz} < \delta_{yy} < \delta_{xx}$) points to the same, bridging or terminal/bridging, coordination mode of the Dtph groups. To determine the structural function of the Dtph groups in complexes **Ia** and **Ib**, the ^{31}P chemical shift anisotropy should be quantified. To do this, we constructed the χ^2 plots (Fig. 3) as a function of ^{31}P chemical shift anisotropy tensor parameters: the chemical shift anisotropy $\delta_{\text{aniso}} = (\delta_{zz} - \delta_{\text{iso}})$ and the asymmetry parameter $\eta = (\delta_{yy} - \delta_{xx})/(\delta_{zz} - \delta_{\text{iso}})$. (The value $\eta = 0$ corresponds to the axially symmetric chemical shift tensor, and the increase in η from 0 to 1 reflects the increase in the rhombic contribution.) It is important that δ_{aniso} is negative for both complexes **Ia** and **Ib** (Table 4). Previously [20], we reported that the sign of δ_{aniso} depends on the SPS angle. For negative δ_{aniso} values, the following correlation is valid: a smaller SPS angle corresponds to a larger $-\delta_{\text{aniso}}$ value (i.e., to a smaller magnitude $|-\delta_{\text{aniso}}|$). Let us compare in this context the δ_{aniso} values for **Ia** and **Ib** and the lead(II) complex $[\text{Pb}\{\text{S}_2\text{P(O-}\textit{cyclo}\text{-C}_6\text{H}_{11})_2\}_2]_n$, in which two structurally nonequivalent Dtph groups have the terminal/bridging function [25]. For these groups, δ_{aniso} is –59.0 and –64.4 ppm and the corresponding SPS angles are 114.14° and 114.35°, respectively [25]. In our case, considerably larger SPS angles are expected for the thallium(I) complexes since $|-\delta_{\text{aniso}}| = 71.5$ (**Ia**) and 94.7 (**Ib**) ppm.

To verify the conclusions made on the basis of ^{31}P CP/MAS NMR data, we determined the molecular and crystal structure of **Ib** by X-ray crystallography.

Table 1. Crystallographic data and experimental and refinement details for structure **Ib** $[\text{Tl}_2\{\text{S}_2\text{P(O-}\textit{cyclo}\text{-C}_6\text{H}_{11})_2\}_2]_n$

Parameter	Value
Empirical formula	$C_{12}H_{22}O_2PS_2Tl$
FW	497.76
Temperature, K	298(2)
Wavelength	MoK_α (0.71073 Å)
System	Monoclinic
Space group	*Pn*
a, Å	10.543(1)
b, Å	12.119(1)
c, Å	26.031(3)
β, deg	96.148(2)
V, Å^3	3306.9(7)
Z	8
$\rho_{\text{calc.}}$, g/cm^3	2.000
μ, mm^{-1}	10.110
F(000)	1904
Crystal shape	Prism (0.304 × 0.062 × 0.035 mm)
θ range, deg	2.57–27.01
Index ranges	$-11 \leq h \leq 13$, $-14 \leq k \leq 15$, $-33 \leq l \leq 33$
Number of measured reflections	20479
Number of unique reflections	11112 ($R_{\text{int}} = 0.0554$)
Number of reflections with $I > 2\sigma(I)$	7990
Refinement method	Full-matrix least squares on F^2
Number of refinement variables	649
GOOF	0.962
R for $F^2 > 2\sigma(F^2)$	$R1 = 0.0446$, $wR2 = 0.1000$
R for all reflections	$R1 = 0.0746$, $wR2 = 0.1144$
Extinction coefficient	Not refined
Flack parameter	0.083(9)
Residual electron density (min/max), e/Å^3	–0.950/2.761

Description of the molecular structure of Ib. The unit cell of crystalline thallium(I) *O,O'*-dicyclohexyl phosphorodithioate comprises eight formula units (Table 1, Fig. 4). The basic structural units of the complex are noncentrosymmetric binuclear molecules $[\text{Tl}_2\{\text{S}_2\text{P(O-}\textit{cyclo}\text{-C}_6\text{H}_{11})_2\}_2]$, two of them being structurally nonequivalent with respect to the other two:

Table 2. Atomic coordinates and isotropic equivalent thermal parameters U_{eq} (Å^2) for complex **Ib**

Atom	x	y	z	U_{eq}	Atom	x	y	z	U_{eq}
Tl(1)	0.67993(3)	0.01452(3)	0.07993(1)	0.0324(1)	C(36)	0.3876(7)	–0.1311(6)	0.2407(4)	0.037(3)
Tl(2)	0.88674(3)	0.24149(3)	0.18469(1)	0.0337(1)	O(4)	0.6836(7)	–0.0238(6)	0.2827(2)	0.047(2)
Tl(3)	0.87900(3)	0.51420(3)	0.07919(1)	0.0321(1)	C(41)	0.7775(7)	0.0122(7)	0.3241(3)	0.041(3)
Tl(4)	0.68888(3)	0.74151(3)	0.18815(1)	0.0296(1)	C(42)	0.7086(10)	0.0490(7)	0.3688(3)	0.066(3)
S(1)	0.9234(3)	0.0582(2)	0.0326(1)	0.0450(8)	C(43)	0.6334(9)	–0.0484(7)	0.3882(4)	0.069(4)
S(2)	0.7554(2)	0.2695(2)	0.0756(1)	0.0306(6)	C(44)	0.7228(9)	–0.1423(8)	0.4033(3)	0.058(3)
S(3)	0.8134(2)	–0.0136(2)	0.1891(1)	0.0319(6)	C(45)	0.795(1)	–0.1809(7)	0.3606(4)	0.063(3)
S(4)	0.6478(3)	0.1970(2)	0.2316(2)	0.0583(9)	C(46)	0.8656(8)	–0.0846(7)	0.3375(4)	0.055(3)
S(5)	0.6268(2)	0.5709(2)	0.0221(1)	0.0351(6)	O(5)	0.5334(5)	0.7734(5)	0.0710(2)	0.028(2)
S(6)	0.8046(2)	0.7685(2)	0.08713(9)	0.0269(6)	C(51)	0.4017(6)	0.7658(6)	0.0473(3)	0.028(2)
S(7)	0.7641(2)	0.4893(2)	0.17923(9)	0.0286(6)	C(52)	0.3566(7)	0.8799(6)	0.0332(4)	0.034(2)
S(8)	0.9416(3)	0.6823(2)	0.2469(1)	0.0381(7)	C(53)	0.2135(7)	0.8800(8)	0.0145(4)	0.046(3)
P(1)	0.8980(2)	0.2178(2)	0.03744(9)	0.0249(6)	C(54)	0.1371(8)	0.8234(6)	0.0527(3)	0.033(2)
P(2)	0.6708(2)	0.0385(2)	0.22689(9)	0.0277(6)	C(55)	0.1831(7)	0.7089(7)	0.0664(4)	0.037(2)
P(3)	0.6482(2)	0.7263(2)	0.04194(8)	0.0215(5)	C(56)	0.3247(7)	0.7100(8)	0.0849(3)	0.039(3)
P(4)	0.9174(2)	0.5287(2)	0.22695(9)	0.0250(6)	O(6)	0.6328(6)	0.8058(5)	–0.0077(2)	0.030(2)
O(1)	0.8880(7)	0.2755(5)	–0.0180(2)	0.038(2)	C(61)	0.6845(6)	0.7820(7)	–0.0561(2)	0.027(2)
C(11)	0.8370(8)	0.2267(8)	–0.0681(3)	0.072(4)	C(62)	0.8272(7)	0.7896(9)	–0.0502(3)	0.040(3)
C(12)	0.8798(9)	0.2998(7)	–0.1098(4)	0.063(3)	C(63)	0.8802(8)	0.7805(8)	–0.1029(3)	0.044(3)
C(13)	0.8172(8)	0.4148(8)	–0.1109(5)	0.078(4)	C(64)	0.8205(8)	0.8638(9)	–0.1404(4)	0.055(3)
C(14)	0.6741(9)	0.404(1)	–0.1144(5)	0.099(5)	C(65)	0.6786(8)	0.863(1)	–0.1459(3)	0.062(3)
C(15)	0.633(1)	0.3372(7)	–0.0706(4)	0.067(4)	C(66)	0.6251(9)	0.8684(8)	–0.0933(3)	0.044(3)
C(16)	0.6956(8)	0.2228(8)	–0.0687(5)	0.069(4)	O(7)	1.0335(5)	0.4804(5)	0.1994(2)	0.030(2)
O(2)	1.0184(5)	0.2803(5)	0.0641(2)	0.030(2)	C(71)	1.1644(6)	0.4848(6)	0.2256(3)	0.027(2)
C(21)	1.1426(6)	0.2731(6)	0.0435(3)	0.024(2)	C(72)	1.2125(7)	0.3685(6)	0.2338(4)	0.030(2)
C(22)	1.2356(7)	0.2158(8)	0.0818(3)	0.042(3)	C(73)	1.3547(7)	0.3661(7)	0.2552(4)	0.041(3)
C(23)	1.3708(7)	0.2176(7)	0.0639(4)	0.047(3)	C(74)	1.4303(8)	0.4321(7)	0.2201(4)	0.048(3)
C(24)	1.4114(8)	0.3344(7)	0.0521(4)	0.045(3)	C(75)	1.3848(7)	0.5501(7)	0.2153(4)	0.045(3)
C(25)	1.3165(7)	0.3879(8)	0.0134(4)	0.046(3)	C(76)	1.2443(7)	0.5513(7)	0.1919(3)	0.038(3)
C(26)	1.1825(7)	0.3874(6)	0.0293(4)	0.037(3)	O(8)	0.9259(6)	0.4458(5)	0.2748(2)	0.032(2)
O(3)	0.5478(5)	–0.0280(5)	0.2030(2)	0.026(2)	C(81)	0.8692(8)	0.4593(8)	0.3218(3)	0.058(3)
C(31)	0.4273(6)	–0.0180(6)	0.2247(3)	0.020(2)	C(82)	0.7334(9)	0.488(1)	0.3176(4)	0.085(4)
C(32)	0.3304(7)	0.0323(8)	0.1845(3)	0.037(3)	C(83)	0.678(1)	0.4937(8)	0.3698(3)	0.060(3)
C(33)	0.1988(7)	0.0346(7)	0.2038(4)	0.043(3)	C(84)	0.7135(8)	0.3908(8)	0.4017(4)	0.054(3)
C(34)	0.1579(7)	–0.0787(7)	0.2208(3)	0.039(3)	C(85)	0.8524(9)	0.370(1)	0.4066(3)	0.087(4)
C(35)	0.2569(7)	–0.1297(8)	0.2601(3)	0.039(3)	C(86)	0.903(1)	0.3592(8)	0.3541(3)	0.058(3)

hereinafter, molecules A, including the Tl(1) and Tl(2) atoms, and molecules B, including the Tl(3) and Tl(4) atoms (Fig. 5). In the dimers, each of the thallium atom is coordinated by the S,S' atoms of one of the Dtph groups (to form four-membered chelate rings [TlS_2P]) and, additionally, by one sulfur atom of a neighboring Dtph group; thus, thallium has CN = 3 (Fig. 5). The anisobidentate character of the Dtph ligands is manifested in that one Tl–S bond in the four-membered chelate ring is on average 0.2 Å shorter than the other. The

Table 3. Bond lengths (d) and bond (ω) and torsion (φ) angles in complex **Ib**

Dimer A				Dimer B			
Bond	d, Å	Bond	d, Å	Bond	d, Å	Bond	d, Å
Tl(1)–S(1)	3.011(3)	S(1)–P(1)	1.958(4)	Tl(3)–S(5)	2.983(3)	S(5)–P(3)	1.960(3)
Tl(1)–S(2)	3.195(2)	S(2)–P(1)	1.990(3)	Tl(3)–S(6)	3.193(2)	S(6)–P(3)	1.987(3)
Tl(1)–S(3)	3.052(3)	S(3)–P(2)	1.985(4)	Tl(3)–S(7)	3.003(3)	S(7)–P(4)	1.988(3)
Tl(1)–S(6)^a	3.255(2)	S(4)–P(2)	1.942(4)	Tl(3)–S(2)	3.237(2)	S(8)–P(4)	1.942(3)
Tl(2)–S(3)	3.192(3)	P(1)–O(2)	1.574(6)	Tl(4)–S(7)	3.173(3)	P(3)–O(5)	1.599(6)
Tl(2)–S(4)	2.965(3)	P(1)–O(1)	1.598(6)	Tl(4)–S(8)	3.013(3)	P(3)–O(6)	1.605(6)
Tl(2)–S(2)	3.042(2)	P(2)–O(3)	1.595(6)	Tl(4)–S(6)	3.033(2)	P(4)–O(7)	1.595(6)
Tl(2)–S(7)	3.266(3)	P(2)–O(4)	1.630(7)	Tl(4)–S(3)^b	3.244(3)	P(4)–O(8)	1.596(6)
Tl(1)···O(5)^a	3.302(6)	O(1)–C(11)	1.478(9)	Tl(3)···O(2)	3.236(6)	O(5)–C(51)	1.461(8)
Tl(1)···O(6)^a	3.406(6)	O(2)–C(21)	1.470(8)	Tl(3)···O(7)	3.394(6)	O(6)–C(61)	1.455(8)
Tl(2)···O(7)	3.285(6)	O(3)–C(31)	1.450(8)	Tl(4)···O(3)^b	3.207(6)	O(7)–C(71)	1.473(8)
Tl(2)···O(8)	3.405(6)	O(4)–C(41)	1.451(9)	Tl(4)···O(5)	3.326(5)	O(8)–C(81)	1.427(9)
Angle	ω, deg	Angle	ω, deg	Angle	ω, deg	Angle	ω, deg
S(1)Tl(1)S(2)	65.74(7)	Tl(1)S(2)Tl(3)	170.37(8)	S(5)Tl(3)S(6)	66.29(6)	Tl(3)S(7)Tl(2)	86.31(6)
S(1)Tl(1)S(3)	94.15(8)	Tl(2)S(2)Tl(3)	86.19(6)	S(5)Tl(3)S(7)	91.96(7)	Tl(4)S(6)Tl(1)^b	87.22(6)
S(2)Tl(1)S(3)	92.81(7)	Tl(1)S(3)Tl(2)	87.01(7)	S(6)Tl(3)S(7)	85.19(6)	Tl(3)S(7)Tl(4)	95.37(7)
S(1)Tl(1)S(6)^a	80.09(7)	Tl(1)S(3)Tl(4)^a	87.09(6)	S(5)Tl(3)S(2)	82.06(6)	Tl(4)S(7)Tl(2)	169.54(8)
S(2)Tl(1)S(6)^a	141.91(6)	Tl(2)S(3)Tl(4)^a	170.14(9)	S(6)Tl(3)S(2)	141.76(6)	Tl(4)S(6)Tl(3)	94.38(6)
S(3)Tl(1)S(6)^a	72.62(6)	S(1)P(1)S(2)	117.3(2)	S(7)Tl(3)S(2)	74.58(7)	S(5)P(3)S(6)	117.9(2)
S(2)Tl(2)S(3)	93.07(7)	O(1)P(1)S(1)	111.7(3)	S(6)Tl(4)S(7)	85.05(6)	O(5)P(3)S(5)	113.3(3)
S(2)Tl(2)S(4)	94.76(9)	O(1)P(1)S(2)	109.5(3)	S(6)Tl(4)S(8)	92.85(7)	O(5)P(3)S(6)	104.5(2)
S(3)Tl(2)S(4)	65.75(7)	O(2)P(1)S(1)	113.2(3)	S(7)Tl(4)S(8)	66.00(6)	O(6)P(3)S(5)	111.5(3)
S(2)Tl(2)S(7)	73.64(6)	O(2)P(1)S(2)	104.2(2)	S(6)Tl(4)S(3)^b	73.01(6)	O(6)P(3)S(6)	109.1(3)
S(3)Tl(2)S(7)	142.71(6)	O(2)P(1)O(1)	99.2(3)	S(7)Tl(4)S(3)^b	141.07(6)	O(5)P(3)O(6)	98.6(3)
S(4)Tl(2)S(7)	80.50(7)	S(4)P(2)S(3)	116.9(2)	S(8)Tl(4)S(3)^b	83.05(7)	S(7)P(4)S(8)	118.2(2)
P(1)S(1)Tl(1)	91.1(1)	O(3)P(2)S(3)	105.8(2)	P(3)S(5)Tl(3)	91.1(1)	O(7)P(4)S(7)	104.0(2)
P(1)S(2)Tl(2)	97.9(1)	O(3)P(2)S(4)	115.0(3)	P(3)S(6)Tl(4)	95.8(1)	O(7)P(4)S(8)	112.7(3)
P(1)S(2)Tl(1)	85.3(1)	O(4)P(2)S(3)	107.4(3)	P(3)S(6)Tl(3)	84.7(1)	O(8)P(4)S(7)	108.1(3)
P(1)S(2)Tl(3)	88.8(1)	O(4)P(2)S(4)	113.6(3)	P(3)S(6)Tl(1)^b	84.1(1)	O(8)P(4)S(8)	113.6(3)
P(2)S(3)Tl(1)	97.4(1)	O(3)P(2)O(4)	95.7(3)	P(4)S(7)Tl(2)	84.4(1)	O(7)P(4)O(8)	98.0(3)
P(2)S(3)Tl(2)	84.8(1)	C(11)O(1)P(1)	127.1(6)	P(4)S(7)Tl(3)	98.1(1)	C(51)O(5)P(3)	120.7(5)
P(2)S(3)Tl(4)^a	88.1(1)	C(21)O(2)P(1)	121.2(5)	P(4)S(7)Tl(4)	85.2(1)	C(61)O(6)P(3)	124.3(5)
P(2)S(4)Tl(2)	92.1(1)	C(31)O(3)P(2)	121.0(5)	P(4)S(8)Tl(4)	90.5(1)	C(71)O(7)P(4)	120.3(5)
Tl(1)S(2)Tl(2)	87.11(6)	C(41)O(4)P(2)	120.5(6)	Tl(3)S(6)Tl(1)^b	168.78(8)	C(81)O(8)P(4)	127.1(6)
Angle	φ, deg	Angle	φ, deg	Angle	φ, deg	Angle	φ, deg
Tl(1)S(1)S(2)P(1)	–171.1(2)	Tl(2)S(3)S(4)P(2)	–171.9(2)	Tl(3)S(5)S(6)P(3)	177.8(2)	Tl(4)S(7)S(8)P(4)	175.4(2)
S(1)Tl(1)P(1)S(2)	–172.3(2)	S(3)Tl(2)P(2)S(4)	–172.9(2)	S(5)Tl(3)P(3)S(6)	178.1(2)	S(7)Tl(4)P(4)S(8)	176.0(2)

Note: Symmetry codes: ^{a} x, y – 1, z; ^{b} x, y + 1, z.

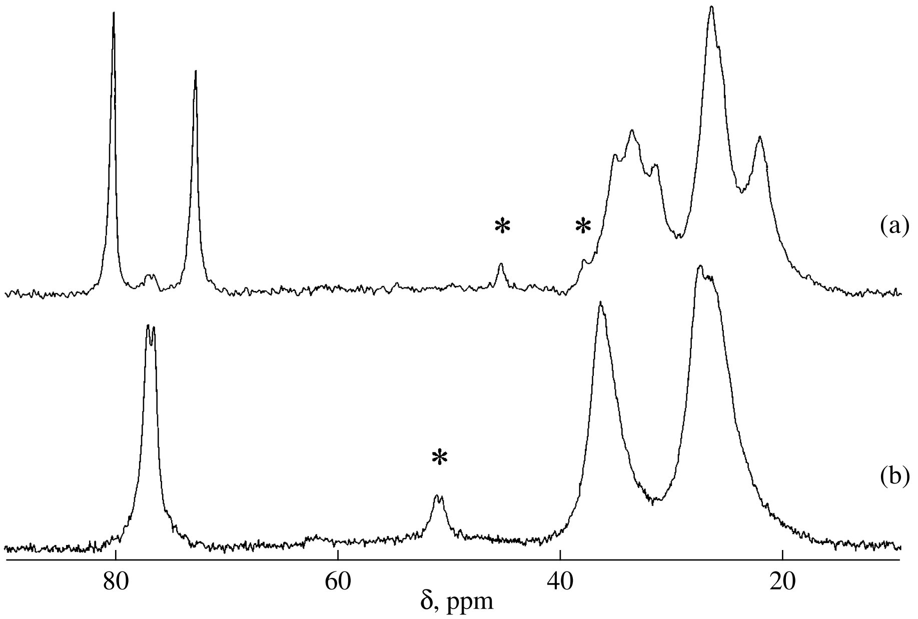

Fig. 1. ^{13}C CP/MAS NMR spectra of two modifications of crystalline thallium(I) *O,O'*-dicyclohexyl phosphorodithioate (a) **Ia** precipitated from an aqueous phase and (b) **Ib** obtained by recrystallization from acetone. Spinning sidebands are marked with asterisks. The scan number/spinning frequency (Hz) were 2720/3200 and 7900/2350, respectively.

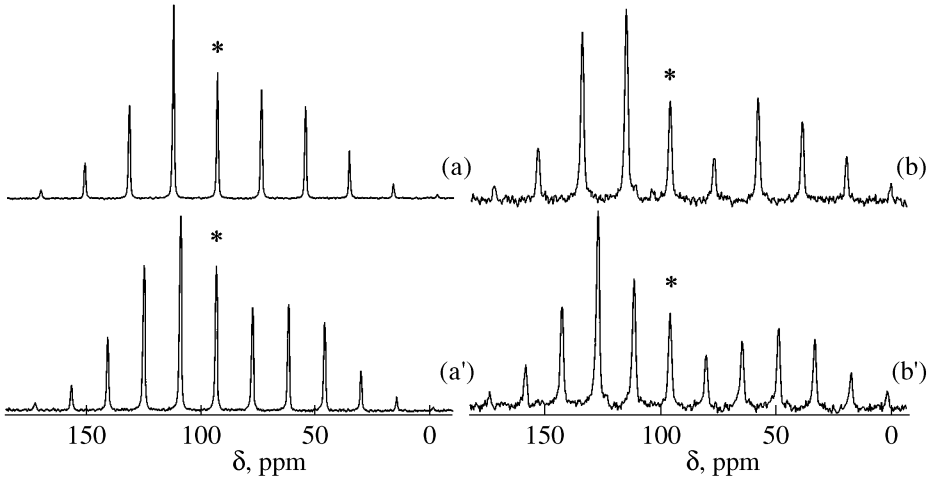

Fig. 2. CP/MAS ^{31}P NMR spectra of two modifications of $[Tl\{S_2P(O\text{-}cyclo\text{-}C_6H_{11})_2\}]_n$: (a, a') **Ia** and (b, b′) **Ib**. The resonance signals in the centers of gravity of the spectra (centerbands) are asterisked. The scan number/spinning frequency (Hz) were (a, b) 32/2800 and (a', b′) 32/2300.

Tl–S bond involving the bridging sulfur atom is considerably stronger than one of the Tl–S bonds in the chelate ring and weaker than the other. The Tl(1) and Tl(2) atoms have additional short contacts with both oxygen atoms of the corresponding Dtph groups in dimers B (Fig. 5, Table 3). At the same time, each of the Tl(3) and Tl(4) atoms has a contact only with one oxygen atom of the Dtph groups in dimers A. However, they also interact with oxygen atoms inside dimers B—O(5) and O(7), respectively.

The geometry of the $[TlS_2P]$ chelate rings in binuclear molecules B is nearly planar since the TlSSP and STlPS torsion angles only slightly differ from 180° (Table 3). Conversely, the atoms of the $[TlS_2P]$ moieties in dimer A exhibit a noticeable tetrahedral deviation from the plane: The above torsion angles are in the

Table 4. ^{31}P NMR parameters of crystalline *O,O'*-dicyclohexyl phosphorodithioates

Compound	^{31}P		
	δ_{iso}, ppm	δ^{*}_{aniso}, ppm	η*
$[Tl\{S_2P(O\text{-}cyclo\text{-}C_6H_{11})_2\}]_n$ (**Ia**)	93.5	–71.5 ± 0.3	0.69 ± 0.01
$[Tl\{S_2P(O\text{-}cyclo\text{-}C_6H_{11})_2\}]_n$ (**Ib**)	96.7	–94.7 ± 0.8	0.35 ± 0.02
$K\{S_2P(O\text{-}cyclo\text{-}C_6H_{11})_2\}$ [20]	109.3 105.0 (1 : 1)	–110.6 ± 1.5 –109.1 ± 1.7	0.14 ± 0.10 0.21 ± 0.06
$[Pb\{S_2P(O\text{-}cyclo\text{-}C_6H_{11})_2\}_2]_n$ [25]	99.6 95.6 (1 : 1)	–59.0 ± 1.1 –64.4 ± 1.2	0.83 ± 0.05 0.88 ± 0.04

* $\delta_{aniso} = \delta_{zz} - \delta_{iso}$; $\eta = (\delta_{yy} - \delta_{xx})/(\delta_{zz} - \delta_{iso})$.

range 171.14°–172.91° (Table 3). The Tl···P and S···S distances in these chelate rings are within 3.599–3.623 and 3.347–3.382 Å, respectively.

The Tl···Tl distance in molecule A (4.2992 Å) is noticeably shorter than in B (4.5683 Å). The thallium polyhedra are distorted tetragonal pyramids with the apical metal atom (the sum of the contiguous STlS angles at the thallium atoms is considerably smaller than 360°). In dimers A and B, the tops of the pyramids are oriented in opposite directions, whereas the tops of the nearest polyhedra in neighboring dimers are oriented in the same direction. Therefore, the interdimeric distances Tl(2)···Tl(3) (4.2922 Å) and Tl(1)···Tl(4)^a (4.3398 Å) are even shorter than the intradimeric distances.

The central eight-membered tricyclic moieties $[Tl_2S_4P_2]$ have a chair conformation (Fig. 5). Comparative analysis of their geometry shows that the angles between the PSSTl and TlSSTl planes in molecule A (85.32° and 85.43°) somewhat differ from the corresponding values in molecule B (84.09° and 85.46°). These structural differences can be explained by the different character of the secondary interactions between the thallium atoms and the oxygen atoms of the alkoxy groups in binuclear molecules A and B (Fig. 5). The differences between molecules A and B, in combination with their considerable structural similar-

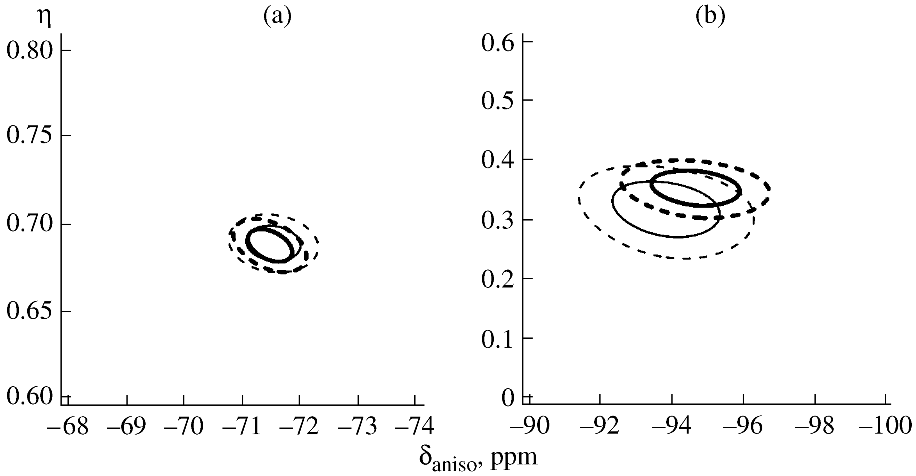

Fig. 3. χ^2 plots (as a function of ^{31}P chemical shift anisotropy parameters) for two modifications of $[Tl\{S_2P(O\text{-}cyclo\text{-}C_6H_{11})_2\}]_n$: (a) **Ia** and (b) **Ib**. The spinning frequencies are 2800 and 2300 Hz (thin and thick lines, respectively). Solid and dashed lines bound the regions of δ_{aniso} and η values at a confidence probability of 68.3 and 95.4%, respectively.

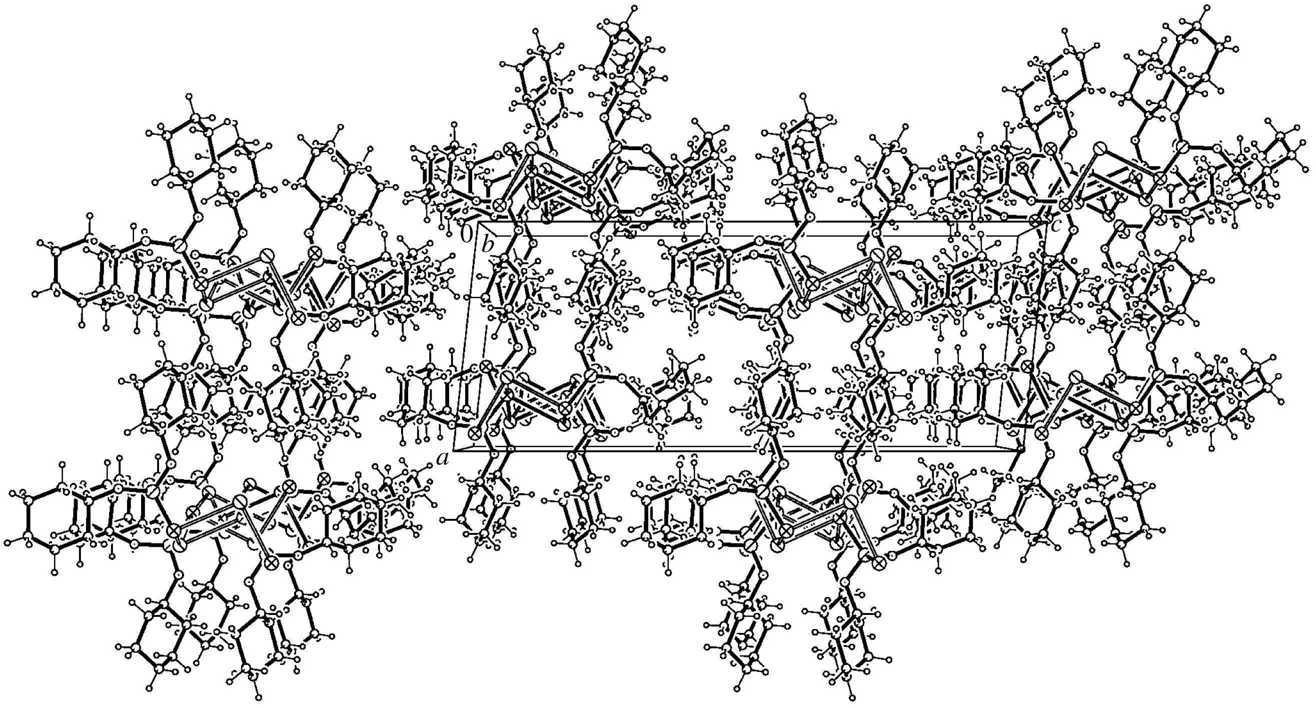

Fig. 4. Crystal packing of structural units in **Ib** (projection onto the *ac* plane).

ity, allow us to treat them as conformers (when a molecular system has two or more coexisting equilibrium spatial forms with close energies).

In binuclear molecules A and B, thallium(I) has a low CN; therefore, further coordinative saturation of thallium in structure **Ib** (to CN = 4) is achieved by additional coordination of sulfur atoms of neighboring molecules (Fig. 5). The sulfur atoms of the Dtph ligands are considerably nonequivalent: one of them forms the bond (the strongest among the Tl–S bonds) only with one thallium atom, whereas the other S atom is involved in coordination with three different thallium atoms. Each binuclear moiety is linked with two neighbors by pairs of ancillary bonds: Tl(1)–S(6)^a (3.255 Å), Tl(2)–S(7) (3.266 Å) and Tl(3)–S(2) (3.237 Å), Tl(4)–S(3)^b (3.244 Å). (Among the Tl–S bonds, these bonds are the weakest ones.) These interactions are responsible for the formation of zigzag polymeric chains of alternating dimers A and B running along the crystallographic *b* axis. The TlTlTl angles in these chains are as follows: Tl(1)Tl(2)Tl(3), 96.50°; Tl(2)Tl(3)Tl(4), 92.67°; Tl(3)Tl(4)Tl(1)^b, 92.13°; Tl(2)Tl(1)Tl(4)^a, 95.84°. It is worth noting that there is considerable structural difference between complex **Ib** and previously described thallium(I) *N,N*-cyclopentamethylene- [4] and *N,N*-cyclohexamethylenedithiocarbamates [7], which also have chain polymer structures. In the latter, the structural units are also binuclear molecules $[Tl_2\{S_2CN(CH_2)_m\}_2]_n$ ($m = 5$ [4] and 6 [7]), but they have a distorted octahedral structure with the apical location of thallium atoms, each of which simultaneously coordinates all four sulfur atoms.

As expected from ^{31}P chemical shift anisotropy data, the SPS angles in the Dtph ligands of compound **Ib** (116.9°–118.2°) are significantly larger than in the lead(II) complex [25]. The phosphorus atoms are in a distorted tetrahedral environment of sulfur and oxygen atoms $[S_2O_2]$. The P–S bond lengths are considerably different: 1.942–1.960 and 1.985–1.990 Å. The former are close to the ideal double bond P=S (1.94 Å), whereas the latter are intermediate between phosphorus–sulfur double and single (2.14 Å) bonds [29]. The geometry of the six-membered rings $–C_6H_{11}$ can be approximated by a chair conformation. The C–C bond lengths and CCC bond angles in the rings vary within 1.47–1.55 Å and 109.0°–114.3°, respectively.

ACKNOWLEDGMENTS

We are grateful to Prof. I.V. Rodushkin for his help with elemental analysis and to CHEMINOVA AGRO, Inc. (Denmark) for supplying potassium *O,O'*-dicyclohexyl phosphorodithioate.

This work was supported by the Russian Foundation for Basic Research (project no. 08-03-00068-a) and the Presidium of the Far East Division of the RAS (project

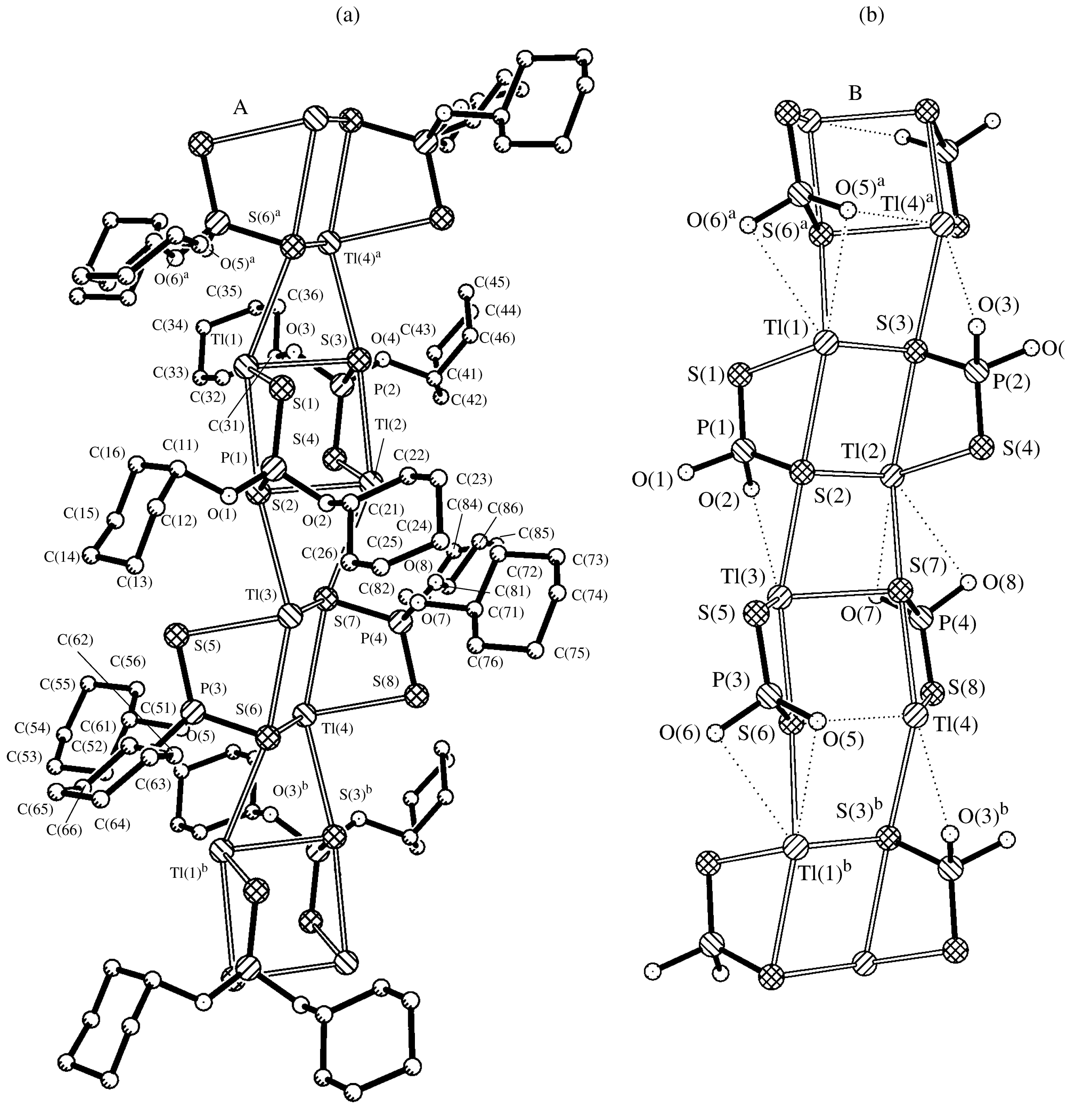

Fig. 5. (a, b) Projections of a fragment of the chain structure of **Ib**. in projection b, alkyl groups are omitted for clarity.

no. 06-III-V-04-099, Basic and Applied Studies of Young Scientists, 2006–2008).

REFERENCES

1. L. Nilson and R. Hesse, Acta Chem. Scand. **23** (6), 1951 (1963).
2. P. Jennische, Å. Olin, and R. Hesse, Acta Chem. Scand. **26** (7), 2799 (1972).
3. H. Anacker-Eickhoff, P. Jennische, and R. Hesse, Acta Chem. Scand. A **29** (1), 51 (1975).
4. A. V. Ivanov, O. A. Bredyuk, A. V. Gerasimenko, and O. N. Antzutkin, Dokl. Akad. Nauk **420** (5), 637 (2008) [Dokl. Phys. Chem. **420** (2), 130 (2008)].
5. H. Pritzkow and P. Jennische, Acta Chem. Scand. A **29** (1), 60 (1975).
6. E. Elfwing, H. Anacker-Eickhoff, P. Jennische, and R. Hesse, Acta Chem. Scand. A **30** (5), 335 (1976).

7. A. V. Ivanov, O. A. Bredyuk, A. V. Gerasimenko, et al., Koord. Khim. **32** (5), 354 (2006) [Russ. J. Coord. Chem. **32** (5), 339 (2006)].
8. P. Jennische and R. Hesse, Acta Chem. Scand. **27** (9), 3531 (1973).
9. S.-H. Hong and P. Jennische, Acta Chem. Scand. A **32** (4), 313 (1978).
10. A. Pines, M. G. Gibby, and J. S. Waugh, J. Chem. Phys. **56** (4), 1776 (1972).
11. W. L. Earl and D. L. VanderHart, J. Magn. Reson. **48** (1), 35 (1982).
12. C. R. Morcombe and K. W. Zilm, J. Magn. Reson. **162** (2), 479 (2003).
13. K. Karaghiosoff, *Encyclopedia of Nuclear Magnetic Resonance*, Ed. by D. M. Grant and R. K. Harris (Wiley, New York, 1996), Vol. 6, p. 3612.
14. W. H. Press, S. A. Teukolsky, W. T. Vetterling, and B. P. Flannery, *Numerical Recipes in C* (Cambridge Univ. Press, Cambridge, 1994).
15. P. Hodgkinson and L. Emsley, J. Chem. Phys. **107** (13), 4808 (1997).
16. O. N. Antzutkin, Y. K. Lee, and M. H. Levitt, J. Magn. Reson. **135** (1), 144 (1998).
17. S. Wolfram, *The Mathematica Book*, 4th ed. (Wolfram Media / Cambridge Univ. Press, Cambridge, 1999).
18. Bruker, *SMART and SAINT-Plus. Versions 5.0. Data Collection and Processing Software for the SMART System* (Bruker AXS, Inc., Madison, Wisconsin, USA, 1998).
19. Bruker, *SHELXTL/PC. Versions 5.10. An Integrated System for Solving, Refining and Displaying Crystal Structures from Diffraction Data* (Bruker AXS, Inc., Madison, Wisconsin, USA, 1998).
20. A.-C. Larsson, A. V. Ivanov, W. Forsling, et al., J. Am. Chem. Soc. **127** (7), 2218 (2005).
21. A. V. Ivanov, A.-C. Larsson, N. A. Rodionova, et al., Zh. Neorg. Chem. **49** (3), 423 (2004) [Russ. J. Inorg. Chem. **49** (3), 373 (2004)].
22. A. V. Ivanov, O. N. Antzutkin, A.-C. Larsson, et al., Inorg. Chim. Acta **315** (1), 26 (2001).
23. A. V. Ivanov, A. V. Gerasimenko, O. N. Antzutkin, and W. Forsling, Inorg. Chim. Acta **358** (9), 2585 (2005).
24. A. V. Ivanov, O. V. Loseva, M. A. Ivanov, et al., Zh. Neorg. Khim. **52** (10), 1697 (2007) [Russ. J. Inorg. Chem. **52** (10), 1595 (2007)].
25. A.-C. Larsson, A. V. Ivanov, O. N. Antzutkin, et al., Inorg. Chim. Acta **357** (9), 2510 (2004).
26. A.-C. Larsson, A. V. Ivanov, K. J. Pike, et al., J. Magn. Reson. **177** (1), 56 (2005).
27. A. V. Ivanov, S. A. Zinkin, A. V. Gerasimenko, et al., Koord. Khim. **33** (1), 22 (2007) [Russ. J. Coord. Chem. **33** (1), 20 (2007)].
28. M. A. Ivanov, O. N. Antzutkin, V. V. Sharutin, et al., Inorg. Chim. Acta **360** (9), 2897 (2007).
29. S. L. Lawton and G. T. Kokotailo, Inorg. Chem. **8** (11), 2410 (1969).